Proceedings of ASME 2024 Conference on Smart Materials, Adaptive Structures and Intelligent Systems
SMASIS2024
September 9-12, 2024, Atlanta, Georgia

SMASIS2024-139559

WAVENUMBER ANALYSIS-BASED MECHANICAL PROPERTY CHARACTERIZATION FOR ADDITIVELY MANUFACTURED THERMOSET COMPOSITES

Bowen Cai
Mississippi State University
MS State, MS

Hunter Watts
Mississippi State University
MS State, MS

Wayne Huberty
Mississippi State University
MS State, MS

Liang Shen
Virginia Tech
Blacksburg, VA

Zhenhua Tian
Virginia Tech
Blacksburg, VA

ABSTRACT

Thermoset materials have begun to be applied in additive composite manufacturing due to their ability to withstand high temperatures without losing structural integrity. Meanwhile, the characterization of mechanical properties for additively manufactured composites is critical for ensuring the material reliability and safety. However, traditional testing methods struggle to accurately and nondestructively characterize additively manufactured composites due to challenges posed by curing processes, microstructural variability, anisotropic properties of thermoset compsoites, and the risk of damaging these materials during evaluation. For characterizing the mechanical properties of additive-manufactured thermoset composites, this paper presents a novel method that combines a nondestructive PZT-LDV guided wave sensing system and a wavenumber analysis that fuses multidimensional Fourier transform with dispersion curve regression. For proof of concept, we performed an experiment using our method to measure a 3D-printed thermoset composite panel. Based on our nondestructive approach, two material properties (shear wave velocity and Poisson's ratio) in multiple directions were successfully determined for the tested panel. We expect this research to introduce a non-contact and efficient method for characterizing various composites and monitoring their property changes after additive manufacturing.

Keywords: additive manufacturing, thermoset material, wavenumber analysis, dispersion curve, mechanical properties characterization

1. INTRODUCTION

Over the past two decades, additive manufacturing technology has exhibited an exponential development trend. Compared to traditional subtractive manufacturing, additive manufacturing has significantly changed the manufacturing process in many industries, such as aerospace, transportation, energy, and even the biomedical field, due to its characteristics of low development costs, high design flexibility, and tool-less processes[1–8]. Among the materials employed in this innovative process, thermoset composite materials stand out due to their exceptional heat resistance and interlaminar strength. Because thermoset composites are often reinforced with fibers such as carbon or glass to enhance structural integrity, this is critical for applications in high-performance, additively manufactured structures[8–10].

However, the usage of thermoset composites from additive manufacturing encounters unique challenges. One significant hurdle is the accurate characterization of mechanical properties, a paramount for ensuring manufactured parts' performance, reliability, and safety [11]. Traditional characterization methodologies, such as tensile, compression, and bending tests, exhibit several deficiencies when applied to thermoset composites fabricated through additive manufacturing[12]. Due to the variable curing processes, microstructural variability, and inherent anisotropic characteristics of thermoset materials, conventional approaches are typically inadequate to capture the complex mechanical behaviors of additive-manufactured composites[11]. Moreover, traditional techniques are predominantly destructive, which escalates production costs for high-value, non-mass-produced components[13].

This article introduces a novel methodology integrating nondestructive guided wave sensing with wavenumber analysis to characterize the mechanical properties of additively manufactured thermoset composite panels. Compared to other traditional methods for mechanical property characterization, our approach is nondestructive, features a large measurement area, and can obtain multi-directional (360-degree) and multi-type (shear wave velocity and Poisson's ratio) mechanical properties of materials by only one test.

In this paper, Section 2 delineates a guided wave sensing system that combines a piezoelectric (PZT) actuator with a laser Doppler vibrometer (LDV) and elaborates on how the collected signals are analyzed using a frequency-wavenumber analysis method. Section 3 presents a proof-of-concept experimental study to characterize a thermoset composite panel fabricated through a fused deposition modeling process.

2. WAVEFIELD ACQUISITION AND ANALYSIS

This section introduces a method for collecting time-space wavefields using a PZT-LDV guided wave sensing system. Next, a multi-directional frequency-wavenumber analysis is used to analyze the collected data and obtain the guided wave dispersion curves in various propagation directions. Finally, the results from the dispersion curve regression will be compared with theoretical results to obtain the mechanical properties of the test sample.

2.1 PZT-LDV guided wave sensing system and wave-field acquisition

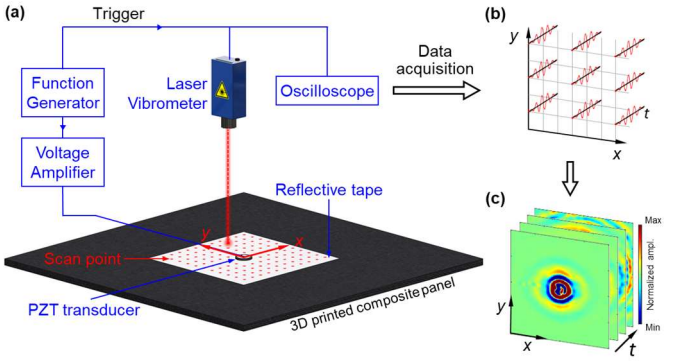

FIGURE 1: SCHEMATIC OF THE PZT – LDV GUIDED WAVE SENSING SYSTEM AND WAVEFIELD ACQUISITION PROCESS.

Guided waves can propagate along waveguides (*e.g.,* thin plates) with low energy loss[14]. By measuring the displacements at multiple surface position of a plate, a guided wave time-space wavefield can be acquired. Figure 1 illustrates a schematic for time-space wavefield collection, including the test setup and measurement process. This study employs a PZT-LDV guided wave sensing system (Fig. 1a) to measure the time-space wavefield. This system comprises two main components: a piezoelectric (PZT) actuator responsible for the excitation of guided waves in the testing part and a laser Doppler vibrometer (LDV) for receiving out-of-plane displacements.

The LDV is vertically mounted on a linear motion stage to collect two-dimensional guided wave signals. A piezoelectric actuator is excited by an amplified chirp signal from a function generator to excite guided waves in the test specimen. The stage controls the LDV to measure waveforms at positions in a user-defined two-dimensional scanning grid (Fig. 1b). The collected waveforms are organized according to their spatial coordinates to form a two-dimensional time-space wavefield u (t, $\mathbf{x}$) (Fig. 1c), a time t and position $\mathbf{x}$ function. The extensive information in the acquired wavefield will be analyzed through a frequency-wavenumber analysis in the following subsection.

2.2 Frequency-wavenumber analysis

To characterize the mechanical properties of composite materials, the challenge can be addressed by measuring the wavenumbers of guided waves at different frequencies and then analyzing their dispersion relationships. Based on the principle that dispersion curves will vary with changes in material properties[15], a multi-directional frequency-wavenumber analysis method is proposed for extracting frequency-wavenumber relation from the acquired time-space wavefield for inversely determining material properties.

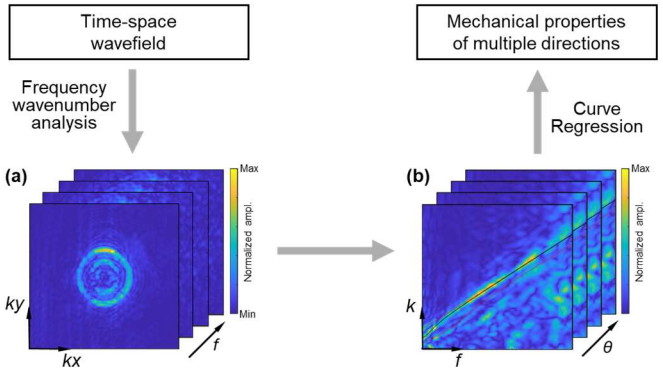

FIGURE 2: DIAGRAM OF THE DISPERSION CURVE FREQUENCY-WAVENUMBER ANALYSIS METHOD.

Figure 2 illustrates a schematic of our analysis method. The time-space wavefield u (t, $\mathbf{x}$), acquired by the guided wave sensing system, can be transformed into a representation in the frequency-wavenumber domain U (f, $\mathbf{k}$) by performing a multidimensional Fourier transform[16–18]:

$$U(f,\mathbf{k}) = \int_{-\infty}^{\infty}\int_{-\infty}^{\infty} u(t,\mathbf{x}) e^{-j(2\pi ft - \mathbf{k}\cdot\mathbf{x})} dt d\mathbf{x}. \quad (1)$$

In this paper, we are more concerned about the distribution of mechanical properties in different directions, so the spatial variables $\mathbf{x}$ can be simplified to 2 dimensions position vector $\mathbf{x} = (x, y)$. Spectra (see Fig. 2a) versus wavenumber $\mathbf{k} = (k_x, k_y)$ at different frequencies can be obtained. These spectra illustrate the relationship between wavenumber values and wave intensities across all propagation directions of guided waves.

To characterize the mechanical properties for each direction, it is necessary to use the experimental dispersion relations from each direction for curve regression. The spatial wavenumber spectrum should be segmented along various angles (radial lines

from the center with k_x=k_y=0). Then, the frequency-wavenumber spectrum for a specific direction can be extracted. By marking the peak wavenumber amplitude at each frequency, an experimental dispersion curve is plotted (see Fig. 2b).

Theoretically, the guided wave frequency-wavenumber dispersion relations can be obtained by solving the following equations[15]:

$$\text{Symmetric modes:} \quad \frac{\tan(qh)}{\tan(ph)} = -\frac{4k^2qp}{\left(k^2-q^2\right)^2} \tag{2}$$

$$\text{Antisymmetric modes:} \quad \frac{\tan(qh)}{\tan(ph)} = -\frac{\left(k^2-q^2\right)^2}{4k^2qp} \tag{3}$$

where, $p^2=(\omega^2/c_L^2)-k^2$, $q^2=(\omega^2/c_S^2)-k^2$, and

$$c_L{}^2 = \frac{1-\upsilon}{(1+\upsilon)(1\text{-}2\upsilon)}\cdot\frac{\mathrm{E}}{\rho}, \tag{4}$$

$$c_S{}^2 = \frac{1}{2(1-\upsilon)}\cdot\frac{E}{\rho}. \tag{5}$$

E, ρ, and υ are the elastic modulus, density, and Poisson's ratio. c_L is the longitudinal wave velocity and c_S is the shear wave velocity. By combining Eq. (4) and (5), we can get an equation showing the c_L and c_S relation:

$$c_L = c_S\sqrt{\frac{2(1-\upsilon)}{1-2\upsilon}} \tag{6}$$

Take Eq. (6) to Eq. (2) and (3), it can be concluded that the guided wave dispersion curves are functions related to c_s and υ.

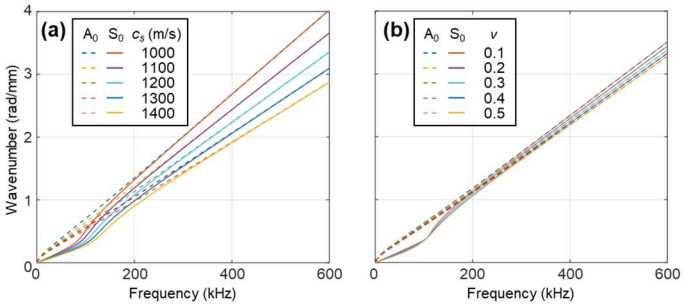

FIGURE 3: THEORETICAL GUIDED WAVE DISPERSION CURVES FOR PLATES WITH DIFFERENT SHEAR WAVE VELOCITIES AND POISSON'S RATIO (a) υ = 0.35, (b) c_S = 1200 m/s.

To observe the changing trends of the dispersion curve under the influence of shear wave velocity and Poisson's ratio, a MATLAB code has been developed to generate a series of theoretical frequency-wavenumber dispersion curves for varying shear wave velocities from 1000 to 1400 m/s and Poisson's ratios from 0.1 to 0.5, within a frequency range of 0 to 600 kHz (see Fig. 3a and b). The code utilizes the guided wave dispersion equations, with shear wave velocity and Poisson's ratio as variables. These theoretical dispersion curves, which correspond to different material properties, allow for comparison with experimental frequency-wavenumber data extracted from the experimental frequency-wavenumber spectra. The best-matched theoretical dispersion curve will be identified through the least squares regression. The regressed shear wave velocity and Poisson's ratio are then considered as the mechanical properties measured by our method.

3. EXPERIMENT VALIDATION

To validate our method, we used a 3D printer to fabricate a thermoset composite panel. Based on the specimen, a proof-of-concept experiment was conducted using the established PZT-LDV sensing system to obtain the sample's time-space wavefield of guided waves. To find the mechanical properties of the specimen, we analyzed the collected wavefields using the frequency-wavenumber analysis method presented in Section 2 and performed dispersion curve regression for material properties evaluation. The experimental results indicate that our method can successfully generate guided waves in thermoset composite panels produced by additive manufacturing and characterize the shear wave velocity and Poisson's ratio.

3.1 Experiments with an additively manufactured thermoset composite panel

The test sample was 3D printed by RAM 48 (MVP, USA), and the printing material was PRD1647 (Polynt, USA) mixed with short carbon fibers. The sample was cut into a 305 × 265 mm plate and then processed using a surface planer to obtain a uniform thickness of 7.9 mm. The composite panel's density is approximately 1050 kg/m³.

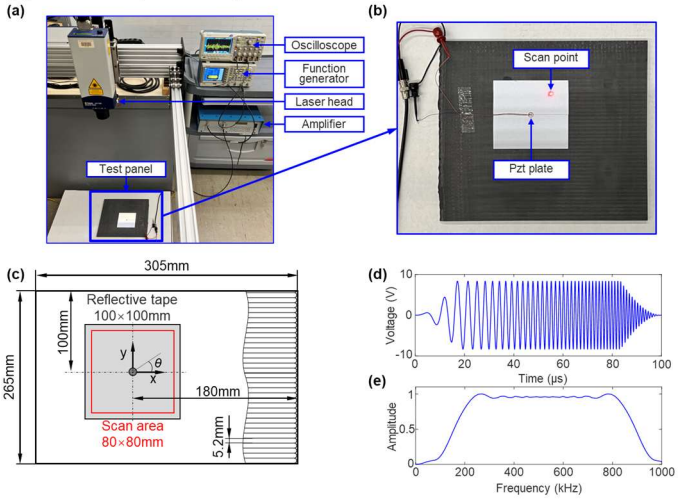

FIGURE 4: EXPERIMENTAL SETUP FOR CHARACTERIZING THE MECHANICAL PROPERTIES OF THE THERMOSET COMPOSITE PANEL.

Figures 4a, b, and c show a photo of the experimental setup, a photo of the test specimen with a piezoelectric actuator and a reflective tape attached, and a schematic of the sensing layout, respectively. To fabricate this specimen, we used a printing

nozzle with a diameter of 5.2 mm and performed printing following a zigzag path by moving the nozzle back and forth along the x-axis . To nondestructively excite guided waves in the test plate, a piezoelectric actuator with a diameter of 7 mm was affixed to the test panel's surface, and the actuator's center position was set as the coordinate origin. The PZT actuator was excited by an arbitrary function generator (AFG3052C Tektronix, USA); the excitation signal was a 50–1000 kHz Hanning-windowed chirp signal and was amplified to 15 Vpp by a voltage amplifier (E&I, USA) (Fig. 4d and 4e). An LDV (OFV-505 Polytec, Germany) was used to acquire the out-of-plane displacement signals of generated guided waves and the time-space wavefield in a predefined 80 mm × 80 mm scanning area with a spatial resolution of 0.8 mm. The sampling frequency was set to 31.25 MHz.

3.2 LDV scanning result and wavefield analysis

The time-space wavefield of guided waves generated by a PZT actuator under the wideband chirp excitation was obtained through laser Doppler vibrometry. Figures 5a to 5d show the wavefields captured by the LDV at 30, 40, 50, and 60 μs, respectively.

Due to the utilization of a chirp signal, the excitation frequency increases with time, leading to the generation of guided waves at different frequencies. From the experimental wavefields, it is observed that the wavefronts have non-circular profiles. This phenomenon suggests that the additively manufactured composite panel is anisotropic, with varying material properties in different directions. Figures 6a to d respectively depict the results of the time-frequency transformation at 200, 300, 400, and 500 kHz frequencies. Wavefields at different frequencies reveal complex guided waves.

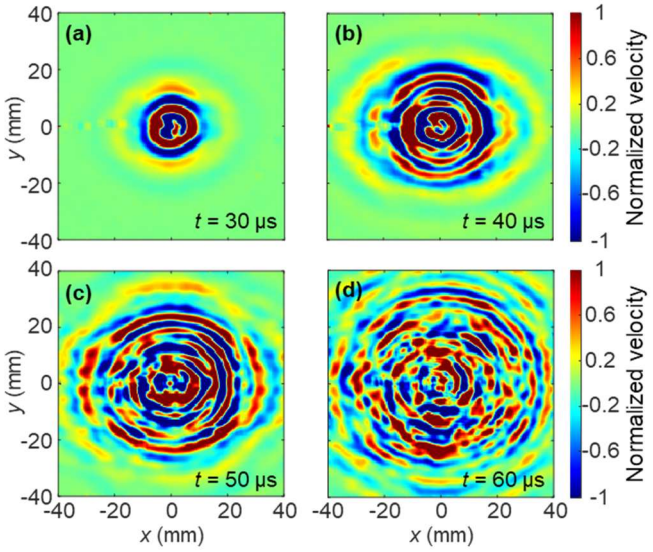

FIGURE 5: ACQUIRED FRAMES OF A TIME-SPACE WAVEFIELD.

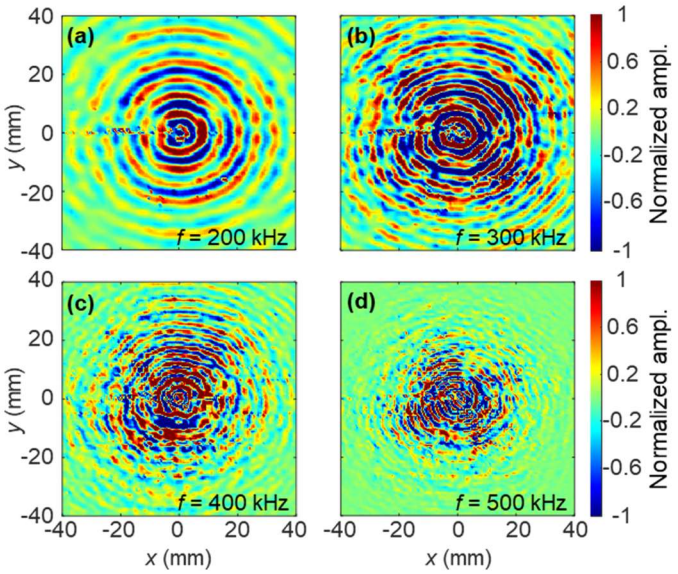

FIGURE 6: FRAMES AT DIFFERENT FREQUENCIES FROM A FREQUENCY-SPACE WAVEFIELD.

3.3 Mechanical properties characterization based on frequency-wavenumber analysis

Employing the method presented in Section 2, a frequency-wavenumber analysis was applied to the acquired time-space wavefield, and two-dimensional wavenumber spectra at various frequencies was generated, as displayed in Figures 7a to d. A circle (white dash line) is overlayed with each spectrum. It can be seen that the wavenumber changes with respect to direction. Moreover, the wavenumber at the 90 degree is higher than the wavenumber at the 0 degree. This increment is likely attributed to the printing path, which is parallel to the x-axis.

For extracting the frequency-wavenumber relations in different directions from the two-dimensional wavenumber spectra at different frequencies, the coordinate system (k_x-k_y) of the spectrum was converted to a polar coordinate system (k_r-θ). Fig. 7e to 7h show extract the frequency-wavenumber spectra for different wave propagation directions θ = 0, 45, 60, and 90 degrees, respectively. Multiple frequency-wavenumber points are further extracted from those spectra, by identifying points with local spectrum intensity peaks. Then, the extracted frequency-wavenumber points are used for inversely determine the material properties through a least square regression-based approach. The searching range for the Poisson's ratio is set to 0.28 to 0.38 [19,20]. This process is implemented in MATLAB, in order to find the theoretical frequency-wavenumber dispersion curve best matching the experimental frequency-wavenumber points for each wave propagation direction. Accordingly, the material properties (υ and c_s) used to calculate the best matching dispersion curve are considered as the properties measured by our method. The characterization results for the four different directions are listed in Table 1.

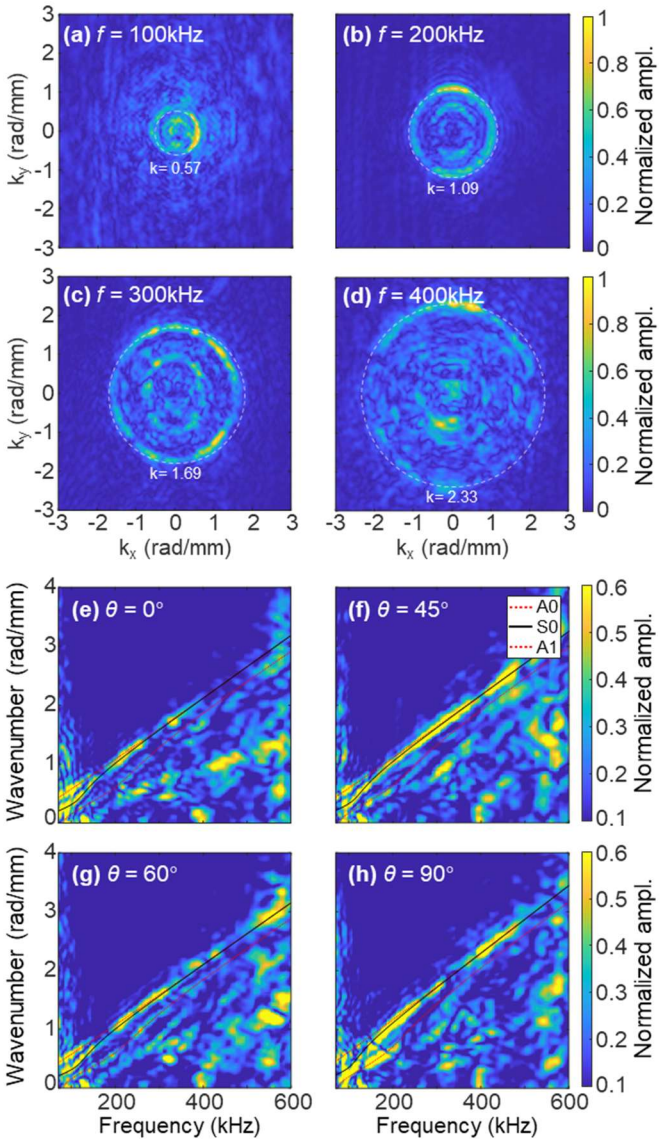

FIGURE 7: 2D WAVENUMBER SPECTRA AT DIFFERENT FREQUENCIES AND FREQUENCY-WAVENUMBER SPECTRA FOR DIFFERENT WAVE PROPAGATION DIRECTIONS.

TABLE 1: EXPERIMENTAL MECHANICAL PROPERTIES FOR DIFFERENT θ

θ (°)	υ	c_s (m/s)
0	0.35	1273.8
45	0.34	1236.2
60	0.34	1264.6
90	0.30	1148.3

Obviously, the shear wave velocity and Poisson's ratio are varied with wave propagation angle θ, with the highest shear wave velocity at the 0 degree and the lowest velocity at the 90 degrees. This phenomenon is consistent with the mechanical performance characteristics of 3D printed products, *i.e.*, strongest performance parallel to the printing direction. Although there are differences in mechanical properties at various angles, the shear wave velocity at 90 degrees reaches 90% of that at 0 degrees, revealing the good interlayer adhesion in our additively manufactured thermoset composite.

3.4 Experiments and results with a 2024 T3 Aluminum Panel

To validate the reliability of our inverse method, we conducted a test using the same approach on a standard 0.75 mm thick 2024-T3 aluminum plate. Since aluminum is an isotropic material, the differences in frequency-wavenumber results for various directions were minimal (Fig. 8). We averaged the mechanical property parameters obtained for different directions to minimize errors and got c_s = 3129.0 m/s and υ = 0.33. The average results showed that the mechanical properties measured by our method were close to the 2024-T3 aluminum's specific properties. Therefore, our experimental results demonstrate that our sensing system and wavenumber analysis method can characterize the mechanical properties of plate-like structures.

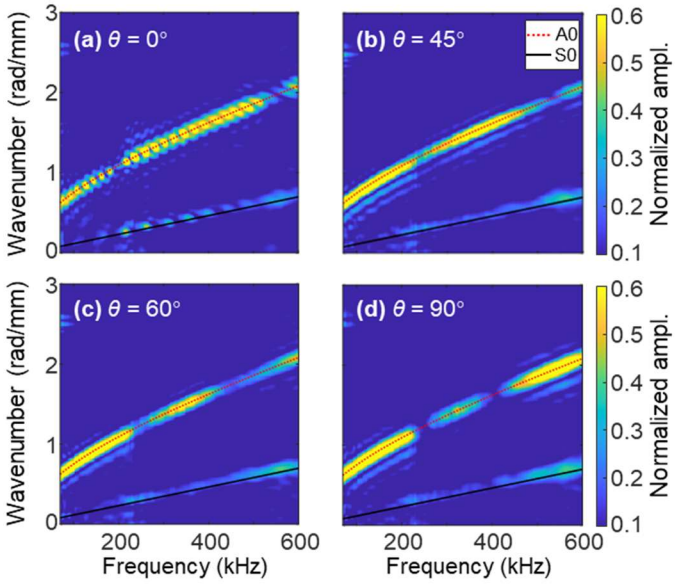

FIGURE 8: FREQUENCY-WAVENUMBER SPECTRA FOR DIFFERENT DIRECTIONS OF AN ALUMINUM PLATE.

4. CONCLUSION

In this paper, a nondestructive method combining a PZT-LDV guided wave sensing system with a frequency-wavenumber analysis method is developed for characterizing the mechanical properties of additively manufactured thermoset composites. This method was demonstrated by characterizing the shear wave velocities and Poisson's ratios for multiple wave propagation directions for an anisotropy thermoset composite. Experimental results demonstrate our method's potential for nondestructively characterizing additively manufactured structures for the quality control of additively manufactured plate-like structures.

ACKNOWLEDGEMENTS

The authors would like to thank the financial support from the Federal Aviation Administration (FAA 12-C-AM-MSU), National Science Foundation (CMMI-2243771 and CMMI-2340016), and DOE Office of Nuclear Energy's Nuclear Energy University Programs (DE-NE0009187).

REFERENCES

[1] R. Mahshid, M.N. Isfahani, M. Heidari-Rarani, M. Mirkhalaf, Recent advances in development of additively manufactured thermosets and fiber reinforced thermosetting composites: Technologies, materials, and mechanical properties, Composites Part A: Applied Science and Manufacturing 171 (2023) 107584.

[2] Y. Wang, Y. Zhou, L. Lin, J. Corker, M. Fan, Overview of 3D additive manufacturing (AM) and corresponding AM composites, Composites Part A: Applied Science and Manufacturing 139 (2020) 106114.

[3] N. Nawafleh, E. Celik, Additive manufacturing of short fiber reinforced thermoset composites with unprecedented mechanical performance, Additive Manufacturing 33 (2020) 101109.

[4] P. Parandoush, D. Lin, A review on additive manufacturing of polymer-fiber composites, Composite Structures 182 (2017) 36–53.

[5] L. Yang, B. Cai, R. Zhang, K. Li, R. Wang, A new type design of lunar rover suspension structure and its neural network control system, Journal of Intelligent & Fuzzy Systems 35 (2018) 269–281.

[6] H. Xiong, M. Zhang, R. Zhang, X. Zhu, L. Yang, X. Guo, B. Cai, A new synchronous control method for dual motor electric vehicle based on cognitive-inspired and intelligent interaction, Future Generation Computer Systems 94 (2019) 536–548.

[7] L. Yang, B. Cai, R. Zhang, K. Li, Z. Zhang, J. Lei, B. Chen, R. Wang, Mechanical Analysis and Performance Optimization for the Lunar Rover's Vane-Telescopic Walking Wheel, Engineering 6 (2020) 936–943.

[8] M.B.A. Tamez, I. Taha, A review of additive manufacturing technologies and markets for thermosetting resins and their potential for carbon fiber integration, Additive Manufacturing 37 (2021) 101748.

[9] K. Deng, C. Zhang, K. (Kelvin) Fu, Additive manufacturing of continuously reinforced thermally curable thermoset composites with rapid interlayer curing, Composites Part B: Engineering 257 (2023) 110671.

[10] F.M. Monticeli, R.M. Neves, H.L. Ornaghi Jr, J.H.S. Almeida Jr, A systematic review on high-performance fiber-reinforced 3D printed thermoset composites, Polymer Composites 42 (2021) 3702–3715.

[11] A. Yadollahi, N. Shamsaei, Additive manufacturing of fatigue resistant materials: Challenges and opportunities, International Journal of Fatigue 98 (2017) 14–31.

[12] T.D. Ngo, A. Kashani, G. Imbalzano, K.T.Q. Nguyen, D. Hui, Additive manufacturing (3D printing): A review of materials, methods, applications and challenges, Composites Part B: Engineering 143 (2018) 172–196.

[13] W. Hao, Y. Liu, H. Zhou, H. Chen, D. Fang, Preparation and characterization of 3D printed continuous carbon fiber reinforced thermosetting composites, Polymer Testing 65 (2018) 29–34.

[14] Z. Tian, L. Yu, Lamb wave frequency–wavenumber analysis and decomposition, Journal of Intelligent Material Systems and Structures 25 (2014) 1107–1123.

[15] V. Giurgiutiu, Structural health monitoring with piezoelectric wafer active sensors, Elsevier/Academic Press, 2008.

[16] B. Cai, T. Li, L. Bo, J. Li, R. Sullivan, C. Sun, W. Huberty, Z. Tian, Development of a piezo stack – laser doppler vibrometer sensing approach for characterizing shear wave dispersion and local viscoelastic property distributions, Mechanical Systems and Signal Processing 214 (2024) 111389.

[17] B. Cai, L. Shen, Z. Pei, T. Li, J. Li, L. Bo, Y. Du, Z. Tian, Development of a Laser Vibrometer-Based Shear Wave Sensing System for Characterizing Mechanical Properties of Viscoelastic Materials, in: American Society of Mechanical Engineers Digital Collection, 2023.

[18] Z. Tian, W. Xiao, Z. Ma, L. Yu, Dispersion curve regression – assisted wideband local wavenumber analysis for characterizing three-dimensional (3D) profile of hidden corrosion damage, Mechanical Systems and Signal Processing 150 (2021) 107347.

[19] K. Shaker, Y. Nawab, A. Saouab, M. Ashraf, A.N. Khan, Effect of silica particle loading on shape distortion in glass/vinyl ester-laminated composite plates, The Journal of The Textile Institute 109 (2018) 656–664.

[20] J. Puentes, J.L. Colon Quintana, A. Chaloupka, N. Rudolph, T.A. Osswald, Moduli development of epoxy adhesives during cure, Polymer Testing 77 (2019) 105863.